

Simulation of mineral precipitation in geothermal installations *The Soultz-sous-Forêts case*

E. Stamatakis^{a,b}, C. Chatzichristos^b,
J. Muller^b, A. Stubos^a and T. Bjørnstad^b

^aNational Centre for Scientific Research Demokritos (NCSR), Athens, Greece

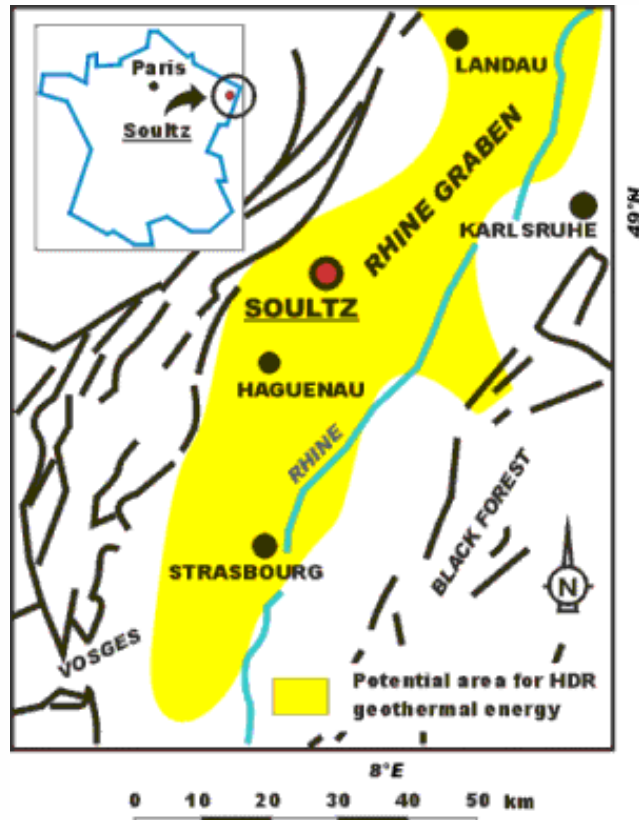
^bInstitute for Energy Technology (IFE), Kjeller, Norway



Outline

- The Soultz-sous-Forêts case
 - Simulation of CaCO_3 scale formation
- The chemical system
- The experimental system
 - Method
 - Typical results
- Mathematical modeling
- Parameter estimation
- Optimal design and operation of the plant

The Soultz-sous-Forêts case



The European HDR-project is situated in Soultz-sous-Forêts, France, at the western border of the Rhine Graben

The geothermal field is a HDR reservoir in northeast France. Its fracture network has been explored down to 5000 m depth. The predicted temperature of 200° C was measured at a depth of 4950 m. The final planned Scientific Pilot Plant module is a 3-well system consisting of one injector and two producers.

The geochemical results obtained during a hydraulic stimulation have been provided to our research group in order to study calcite scaling tendency.



Simulations of CaCO_3 scale formation

The overall objective is the scaling management optimization (optimize the surface processes in order to minimize the impact of calcite scaling).

The only parameter available for optimization is the pressure.

(GPK1)

Source_hot1
Heat_pipe_tubular001
150°C?, 20 kg/s?

10-15 bar, (pipes PN40)

Source_hot2
Heat_pipe_tubular002

(GPK2)

Junction001

Heat_pipe_tubular003

Heat_pipe_tubular004

20°C, 3.5 bar

200-300 m³/h

plate_heat_exchanger002

plate_heat_exchanger001

Sink_hot
(GPK3)

Source_cold

Sink_cold

Designed topology of Soultz geothermal plant using gPROMS



The chemical system

- The main complication is the occurrence of CO₂(g) in reaction [1]. The molar volume of CO₂(g) varies greatly with both temperature and pressure.



The temperature and pressure dependence of these equilibria is given from the work of Atkinson & Mecik (1994*, 1997**).

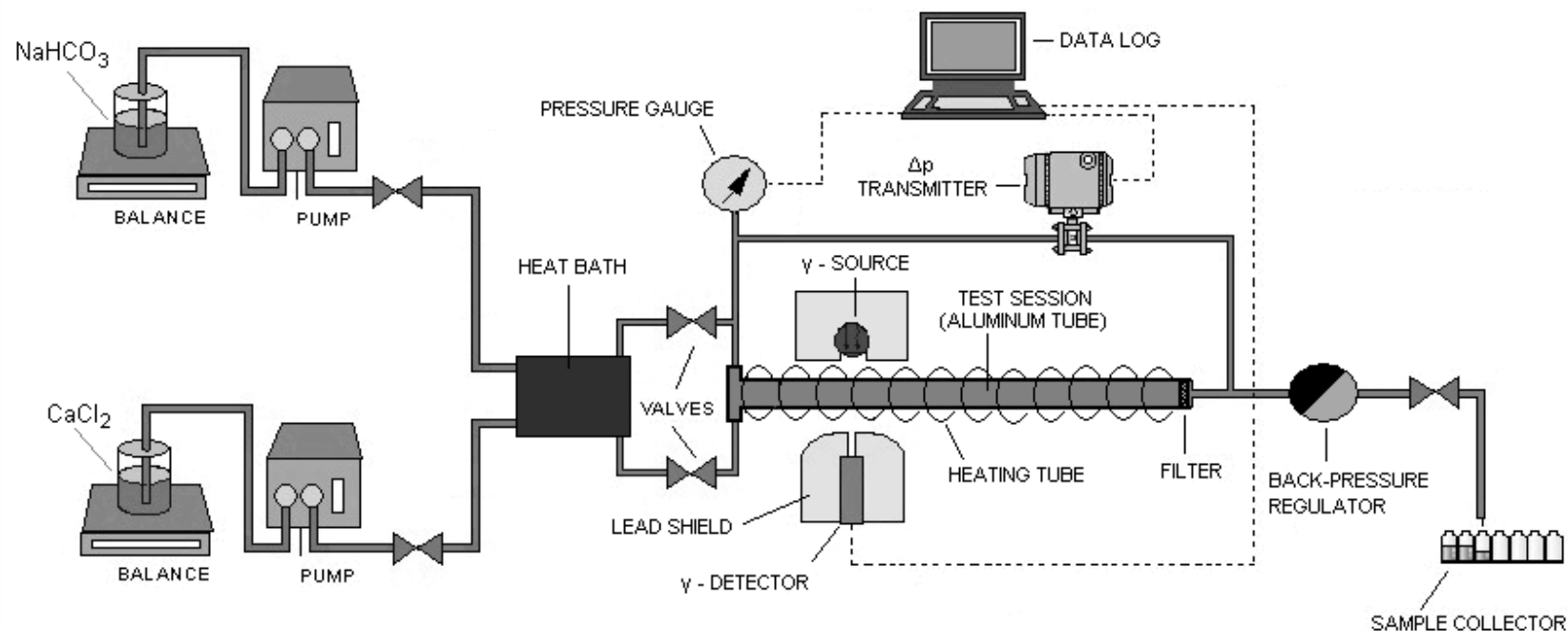
*Atkinson G., Mecik M., “CaCO₃ scale formation: How do we deal with the effects of pressure?”, *Conf. Corrosion 94.*, **Paper 610**, 12pp. (1994).

Atkinson G., Mecik M., “The chemistry of scale prediction”, *J. Petrol. Sci. Eng.*, **17, 113-121 (1997).

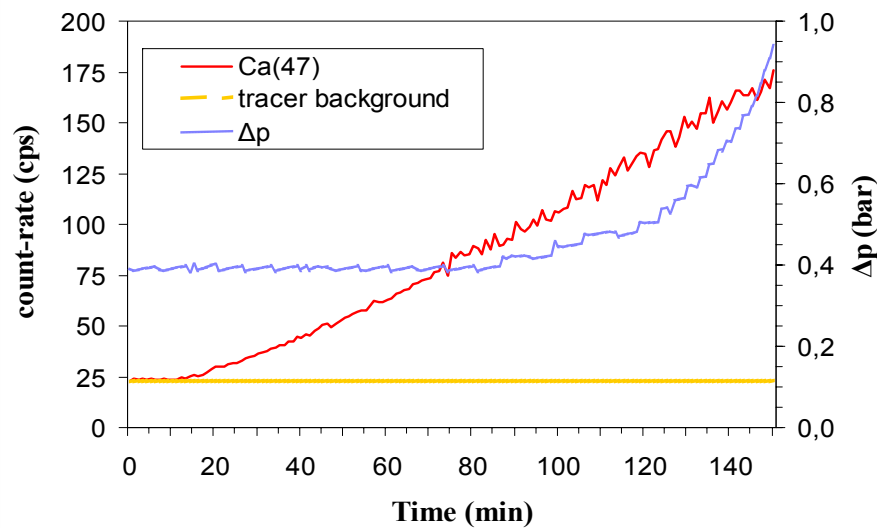


The experimental system

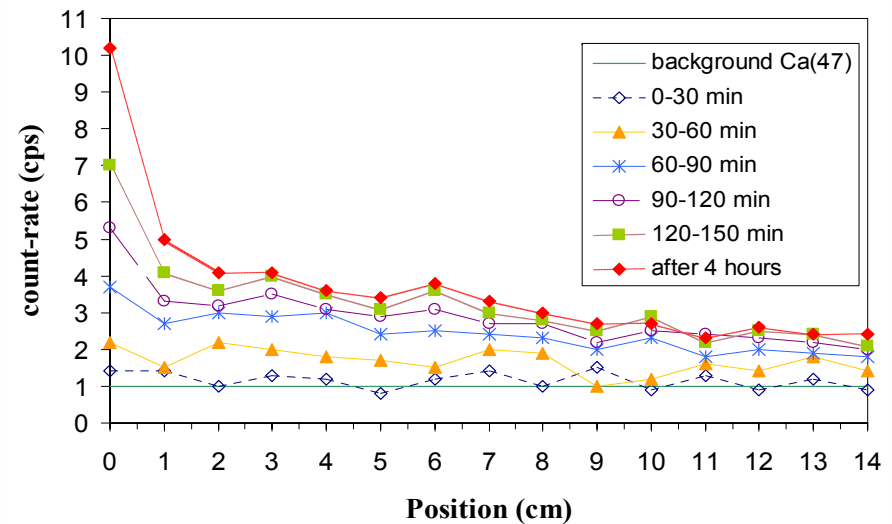
1. Gamma emission based on radioactive tracers added to the flowing and reacting system
2. Gamma transmission based on use of external gamma sources



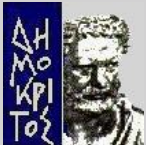
Typical gamma-emission results



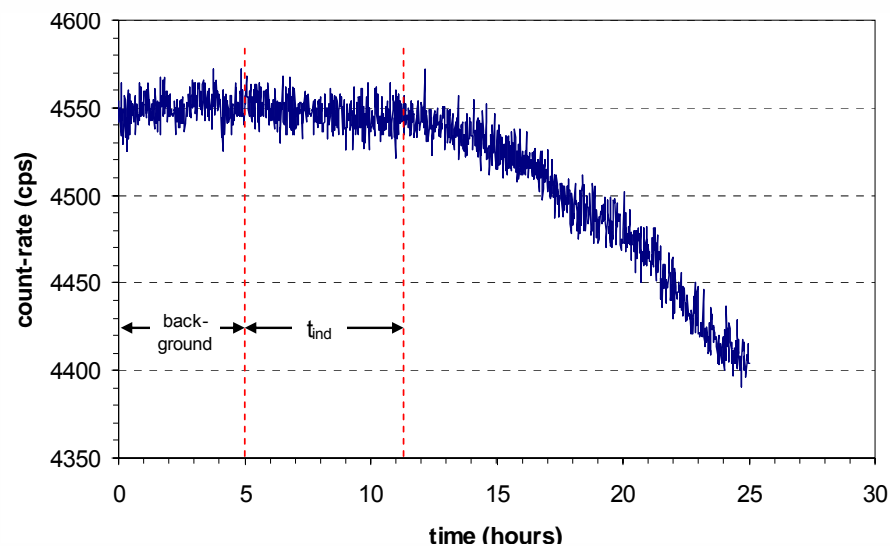
^{47}Ca deposit growth at the inlet and Δp buildup along the tube vs. time



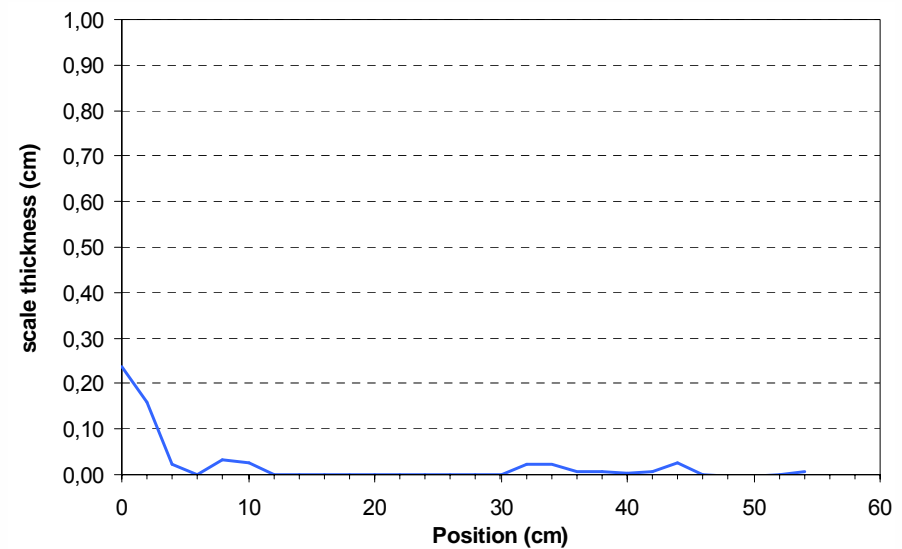
^{47}Ca deposit distribution across the tube at different time-steps



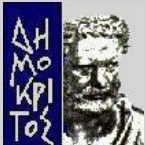
Typical gamma-transmission results



Gamma attenuation measurements for calcite precipitation at the inlet of the tube at 160°C, 15 bars and SR=1.5 (run 2)

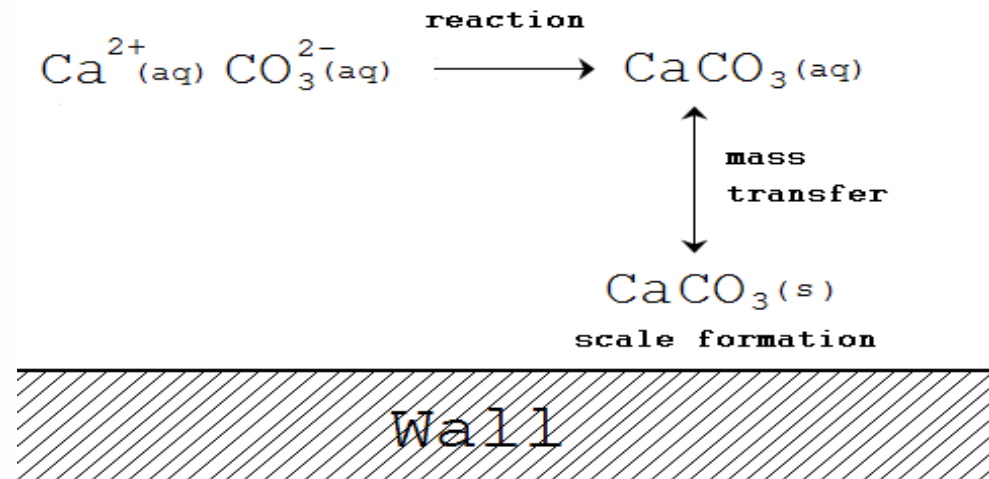


Scale thickness distribution across the tube at the end of run 3



Mathematical modeling

- The key step in studying fouling is to capture the interrelationship between the chemical reactions, which give rise to deposition and the fluid mechanisms encountered along the flow path.
- Here, the necessary heat and mass transfer equations are coupled with the equations which describe the formation of calcite deposits in the transfer pipelines and heat exchanger.
- The overall model involves a coupled set of partial and ordinary differential and algebraic equations which can be described in gPROMS using its distributed process modelling capabilities.



The reaction/mass transfer scheme

Mathematical modeling (2)

Simple models are used to account for the hydro and thermo-dynamic characteristics of the fluid with two common assumptions:

- The fluid temperature in the bulk and thermal layer are radially uniform, i.e. the temperature in the bulk and thermal boundary layer are equal and do not change with the tube radius.
- The fluid flows in plug flow at uniform velocity. The velocity in the thermal boundary layer is assumed negligible in comparison.

Mathematical modeling (3)

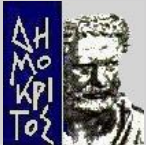
The simplified one-phase flow case in a circular tube

- The material balance for e.g. CaCO_3 in the control volume is given from:

$$\frac{\partial C_{\text{CaCO}_3}}{\partial t} + u_z \frac{\partial C_{\text{CaCO}_3}}{\partial z} = \underbrace{-K_p C_{\text{Ca}}}_{\text{Reaction rate term}} - \underbrace{\left[k_{m\text{CaCO}_3} (C_{\text{CaCO}_3(s)} - C_{\text{CaCO}_3(aq)}) + k_w C_{\text{CaCO}_3(s)} \right]}_{\text{Mass transfer}} + \underbrace{\frac{\partial}{\partial z} \left(D_{\text{CaCO}_3} \frac{\partial C_{\text{CaCO}_3(s)}}{\partial z} \right)}_{\text{diffusion at the axial distance}}$$

- The energy balance (for the heat exchanger) has the form:

$$\frac{\partial T_s}{\partial t} + u_z \frac{\partial T_s}{\partial z} = - \frac{1}{\rho C_{pw}} U a_s (T_s - T_{cold})$$



Quantifying fouling

The rate of deposition is related to the concentration of $\text{CaCO}_3(\text{s})$ by the mass transfer coefficient k_w . The Biot number is used to express the change of heat transfer due to fouling and it is related to the rate of deposition according to:

$$\frac{\partial Bi}{\partial t} = \beta k_w C_{\text{CaCO}_3}, \quad \beta \text{ is a constant}$$

- Deposit thickness and mass at each position z along the heat exchanger:

$$x_d(z) = \frac{\lambda_d Bi(z)}{U_o},$$

$$\text{mass}(z) = \frac{\lambda_d Bi(z)}{U_o} \rho_d$$

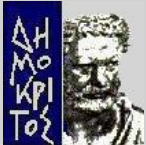
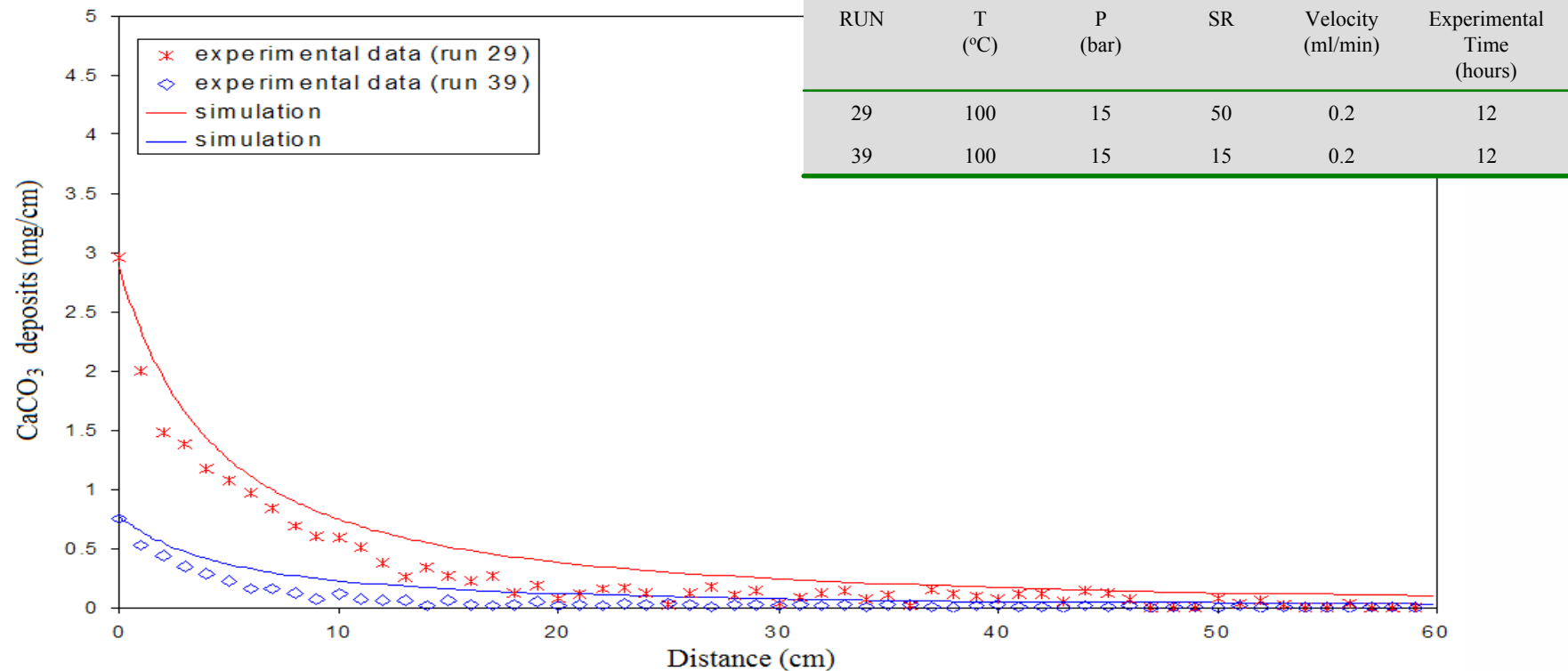


Parameter estimation

- Before using the model to predict the dynamic behaviour of the process, we need to validate it and estimate the values of several unknown model parameters based on the data gathered from our experimentations.
- This type of analysis can be easily performed using the built-in parameter estimation capabilities of gPROMS.
- Thus, the mathematical model is used to estimate the values of the unknown parameters, such as heat transfer coefficients, that best match the experimental data over time.

Preliminary simulation results

- Here, for the purpose of parameters estimation and verification we tried to simulate two specific experimentations.



Optimal design and operation of the plant

- Fouling in geothermal installations is a major problem and, virtually, represents additional costs to the industrial sector such as:
 - capital cost due to cleaning equipment and services
 - lost of production
 - waste of energy and heat
- A detailed economic objective function is going to be used to account for all the important factors related with calcite precipitation and a number of operating constraints will be imposed.

Optimal design and operation of the plant (2)

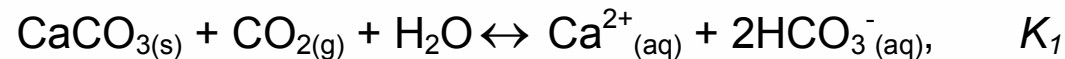
- There are two main issues which must be taken into consideration when establishing optimal control strategies for this problem. The first issue is to ensure that no precipitation occurs and the system operates above its bubble point at all times. The second issue is to seek for the best economic performance.
 - The complexity of the dynamic optimization problem arises primarily from the distributed and highly nonlinear nature of the system model
 - Because of the complexity of the underlying physical process, it is often difficult to define simple strategies in order to address all important issues and take at the same time into account all operating constraints

Thank you!

Temperature-dependent constants for $\ln k$

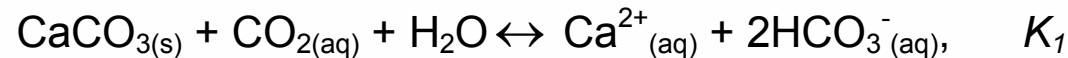
$$\ln k = \frac{\Delta A \ln T}{R} + \frac{\Delta B T}{2R} + \frac{\Delta C}{2RT^2} - \frac{\Delta I_h}{RT} - \frac{\Delta I_g}{R}, \quad (T \text{ in K})$$

Solid	ΔA	ΔB	$\Delta C (\times 10^{-6})$	ΔI_h	ΔI_g
Calcite	-239.623	0.18866	9.0767	83810.8	-1540.62



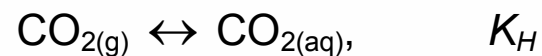
Range: 0 - 300°C

Calcite	282.476	-0.7958	-14.5318	-102360	1772.44
---------	---------	---------	----------	---------	---------



Range: 0 - 200°C

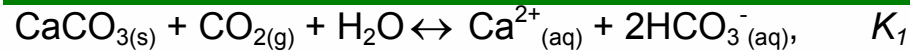
	-80.384	0.18166	6.1255	31661.2	-495.94
--	---------	---------	--------	---------	---------



Range: 0 - 250°C



Effect of pressure on CaCO_3 dissolution



$$\ln \left[\frac{K_P}{K_1} \right] = \frac{-[\Delta \bar{V}_{s,1}^0 - \Delta \bar{V}_{\text{CO}_2(g)}^0]}{RT} (P-1) + \frac{\Delta \bar{K}_{s,1}^0}{2RT} (P^2 - 1)$$

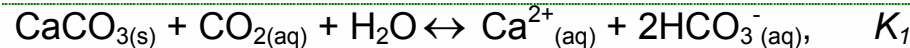
$$\Delta \bar{V}_{s,1}^0 = -26.69 + 0.146365t - 15.7085 \times 10^{-4} t^2 - 1.0566 \times 10^{-6} t^3$$

$$\Delta \bar{K}_{s,1}^0 \times 10^{-3} = 11.8837 + 2.853 \times 10^{-2} t - 8.5531 \times 10^{-4} t^2 + 5.3145 \times 10^{-6} t^3$$

$\Delta \bar{V}_{\text{CO}_2(g)}^0$ from interpolation of the CO_2 molar volumes reported by Angus et al. (1976)

$\Delta \bar{V}_{s,1}^0$ in $\text{cm}^3 \text{mol}^{-1}$, $\Delta \bar{K}_{s,1}^0$ in $\text{cm}^3 \text{bar}^{-1} \text{mol}^{-2}$, t in $^{\circ}\text{C}$

Range: 0 - 150 $^{\circ}\text{C}$, 1 - 200bar



$$\ln \left[\frac{K_P}{K_1} \right] = \frac{-\Delta \bar{V}^0}{RT} (P-1) + \frac{\Delta \bar{K}^0}{2RT} (P^2 - 1)$$

$$\Delta \bar{V}^0 = -61.9 + 20.231 \times 10^{-2} t - 24.45 \times 10^{-4} t^2 - 0.603 \times 10^{-6} t^3$$

$$\Delta \bar{K}^0 \times 10^{-3} = 13.517 + 3.222 \times 10^{-2} t - 15.1385 \times 10^{-4} t^2 + 12.919 \times 10^{-6} t^3$$

$\Delta \bar{V}^0$ in $\text{cm}^3 \text{mol}^{-1}$, $\Delta \bar{K}^0$ in $\text{cm}^3 \text{bar}^{-1} \text{mol}^{-1}$, t in $^{\circ}\text{C}$

Range: 0 - 225 $^{\circ}\text{C}$, 1 - 2000bar

